

## STRAIN RATE BEHAVIOUR OF THREE ROCKS IN TENSION

E. C a d o n i, S. A n t o n i e t t i, M. D o t t a, D. F o r n i

**University of Applied Sciences of Southern Switzerland**  
**DynaMat Laboratory**  
Switzerland

The paper presents the dynamic characterization in tension of three rocks under medium and high strain-rates. The tests have been carried out by means of the JRC-Split Hopkinson Tension Bar and an Hydro-Pneumatic Machine, installed in the DynaMat Laboratory of the University of Applied Sciences of Southern Switzerland. The dynamic direct tension tests have been performed at 3 different strain rates (0.1, 10, 100 strain/second) on an orthogneiss, for loading directions  $0^\circ$ ,  $45^\circ$  and  $90^\circ$  respect to the schistosity, and two different types of marble. Results of the tests show a significantly strain-rate sensitive behaviour, exhibiting dynamic tensile strength increasing with strain-rate. In order to describe the strain rate behaviour of these rocks, the dynamic increase factors in function of the strain rates for tensile strength have been used.

### 1. INTRODUCTION

The mechanical response of rocks under high loading rates is of fundamental importance in tunnel constructions and mining works. The dynamic loading is generated by impact loading of the tools of specialized excavation machines and/or by controlled explosions. The knowledge of the real material constitutive relationships can allow the optimization of the explosive charge and consequent pressure wave amplitude and duration. This fact is important both for economic reasons, to obtain the desired effect with the lowest cost, and for safety measures, in order to avoid risks of heavy vibrations, especially in case of underground excavations in urban areas.

The modern tools used in design and assessment of constructions (i.e. FE codes) require more and more advanced data, as for example the complete stress versus strain curves, until fracture of the rock materials or the implementation of different material constitutive laws. These data have to be measured by means of specialized apparatus able to properly measure the characteristics of the materials. In particular, at high strain rates it is necessary to generate a stress wave pulse well controlled in amplitude and duration, as well as at medium strain rates, the vibration of the systems should be under control. The dynamic

tension test is normally obtainable by Split Hopkinson Pressure Bar (SHPB) device, in the strain range of  $10^2$ – $10^3$  s $^{-1}$ . With this apparatus only indirect measurement of the tensile strength can be available, because it works in compression (splitting test, spalling test, etc.). Some modifications were used by different authors in order to obtain direct pulse [1–4] for rock-like materials as concrete.

The dynamic direct tensile test has been obtained using a modification of the previous apparatus [5–7] for the characterization of concrete and rocks [8–10].

The dynamic direct tensile strength of an orthogneiss has been measured at 3 different strain rates (0.1, 10, 100 strain/second) for loading directions  $0^\circ$ ,  $45^\circ$  and  $90^\circ$  with respect to the schistosity. The two marbles have been characterized at three strain rate regimes: quasi-static, medium and high strain rates.

The tests have been carried out by means of the JRC-Split Hopkinson Tension Bar and the JRC-Hydro-Pneumatic Machine, installed in the DynaMat Laboratory of the University of Applied Sciences of Southern Switzerland.

## 2. EXPERIMENTAL PROGRAM

Static and dynamic loading tests have been conducted on cylindrical rock specimens (diameter = 20 mm, height/diameter = 1). In the case of orthogneiss, series of cores have been drilled out in three directions: the first parallel ( $\theta = 0^\circ$ ) and the second perpendicular ( $\theta = 90^\circ$ ) to the plane of schistosity, the third sampling direction oriented at  $\theta = 45^\circ$  to the plane of schistosity. As a result  $\theta$  is then defined as the angle of schistosity with the loading direction, as shown in Fig. 1.

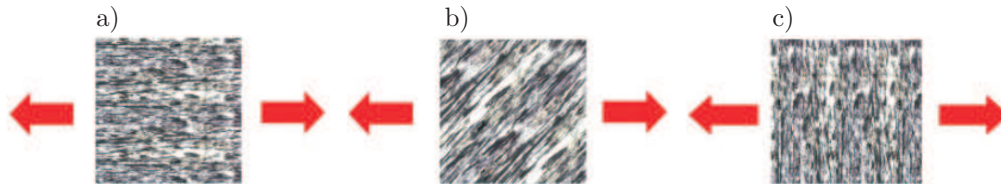


FIG. 1. Loading direction to the schistosity plane: a)  $\theta = 0^\circ$ , b)  $\theta = 45^\circ$ , c)  $\theta = 90^\circ$ .

### 2.1. Materials

The rock materials used for testing are two rocks from the Swiss Alps and the well-known Carrara marble. The Swiss rocks are an orthogneiss from the Onsernone Valley and a Peccia marble from the Maggia Valley of the Canton Ticino (Switzerland). They belong to the group of the metamorphous rocks.

The petrography of the Onsernone orthogneiss is characterized by the presence of white feldspar (albite) and transparent quartz appear in the light min-

erals, as well as are also included a relatively large quantity of white mica (muscovite) and dark mica (biotite), even if this is not evenly distributed. The mean grain size of the crystals is about 0.5 mm while the maximum grain size is 1 mm (see Fig. 2a).

The two marbles are characterized by a granoblastic structures, the Peccia marble (see Fig. 2b) present larger size of grain (about 1 mm) with respect to the Carrara marble (see Fig. 2c), having maximum grain size of about 0.2 mm.

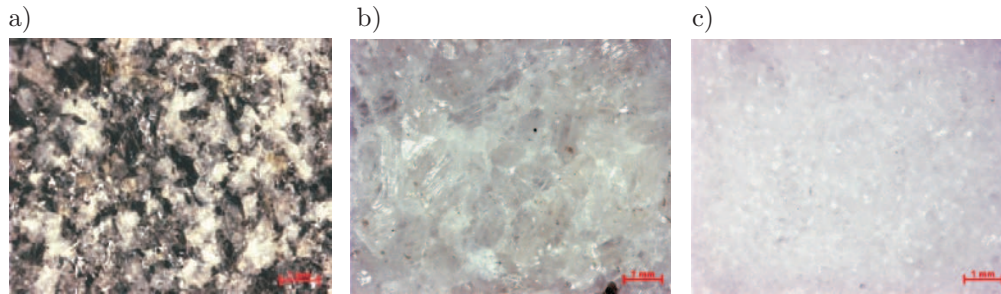


FIG. 2. Microcrystalline structure of the: a) Onsernone orthogneiss, b) Peccia marble, c) Carrara marble.

In order to compare dynamic and quasi-static regime directly, excluding the results of any size effect influence, tensile static tests has been measured on 20 mm diameter 20 mm high specimens (the same geometry of the dynamic tests).

The results of the material characteristics are summarized in Table 1.

Table 1. Mechanical characteristics.

Rock material	Apparent density [kg/m <sup>3</sup> ]	Absolute density [kg/m <sup>3</sup> ]	Young's modulus [GPa]	Compression strength [MPa]	Tensile strength [MPa]
Onsernone orthogneiss	2710	2740	39.3 ( $\theta = 0^\circ$ )	189±8 ( $\theta = 0^\circ$ ) 203±7 ( $\theta = 90^\circ$ )	12.6±0.5 ( $\theta = 0^\circ$ ) 6.1±0.8 ( $\theta = 45^\circ$ ) 2.6±1.1 ( $\theta = 90^\circ$ )
Peccia marble	2706	2795	64.6	87±8	3.9±0.4
Carrara marble	2677	2720	–	79±1	2.0±0.5

### 3. EXPERIMENTAL SET-UPS FOR DYNAMIC TESTING

#### 3.1. The JRC-Split Hopkinson Tensile Bar (JRC-SHTB)

The JRC-SHTB used for rocks characterization at high strain rate consists of two circular aluminum bars, called input and output bars, having respectively the length of 3 m and 6 m, with a diameter of 20 mm, to which the specimen

is glued by using a bi-component epoxy resin. The input bar is connected with a high strength steel pre-tensioned bar 6 m in length, used as pulse generator with a diameter of 12 mm in order to obtain the same acoustical impedance of the input bar, so that the pulse reflection, due to the interface, is avoided.

With reference to Fig. 3, a test with the JRC-SHTB is performed as follows:

- a) first a hydraulic actuator (1), of maximum loading capacity of 600 kN, is pulling the pre-tension high strength steel bar (2); the pre-tension stored in this bar is resisted by the blocking device (3);
- b) second operation is the rupture of the fragile bolt in the blocking device which gives rise to a tensile mechanical pulse of 2.4 ms duration with linear loading rate during the rise time, propagating along the input (4) and output (7) bars, bringing to fracture the specimen (6).

The pulse propagates along the input bar with the velocity  $C_0$  of the elastic wave with its shape remaining constant. When the incident pulse ( $\varepsilon_I$ ) reaches the rock specimen, part of it ( $\varepsilon_R$ ) is reflected by the specimen whereas another part ( $\varepsilon_T$ ) passes through the specimen propagating into the output bar.

The relative amplitudes of the incident, reflected and transmitted pulses, depend on the mechanical properties of the specimen. Strain-gauges glued on the input and output bars of the device are used for the measurement of the elastic deformation (as a function of time), created on both half-bars respectively by the incident/reflected and transmitted pulses.



FIG. 3. High strain-rate tensile tests on specimen  $\varnothing = 20$  mm.

This modified system still satisfies the condition of applicability of the uni-axial elastic wave propagation theory because the pulse wavelength (in order of a few meters) is much higher than the transverse length of the bar (20 mm), so the stress-strain history can be obtained by the following equations:

$$(3.1) \quad \sigma(t) = E_0 \frac{A_0}{A_s} \varepsilon_T(t),$$

$$(3.2) \quad \varepsilon(t) = -\frac{2 \cdot C_0}{L_s} \int_0^t \varepsilon_R(t) dt$$

where  $L_s$  – specimen length;  $A_s$  – specimen cross-section area;  $A_0$  – output bar cross-section area;  $t$  – time.

### 3.2. The Hydro-Pneumatic Machine (HPM)

The medium strain rate tests have been carried out by means of a Hydro-Pneumatic Machine (HPM). The employed HPM is shown in Fig. 4. At the beginning of the test, a sealed piston divides a cylindrical tank in two chambers; one chamber (4) is filled with gas at high pressure (e.g. 150 bars), the other one (5) is filled with water. At the beginning, equal pressure is established in

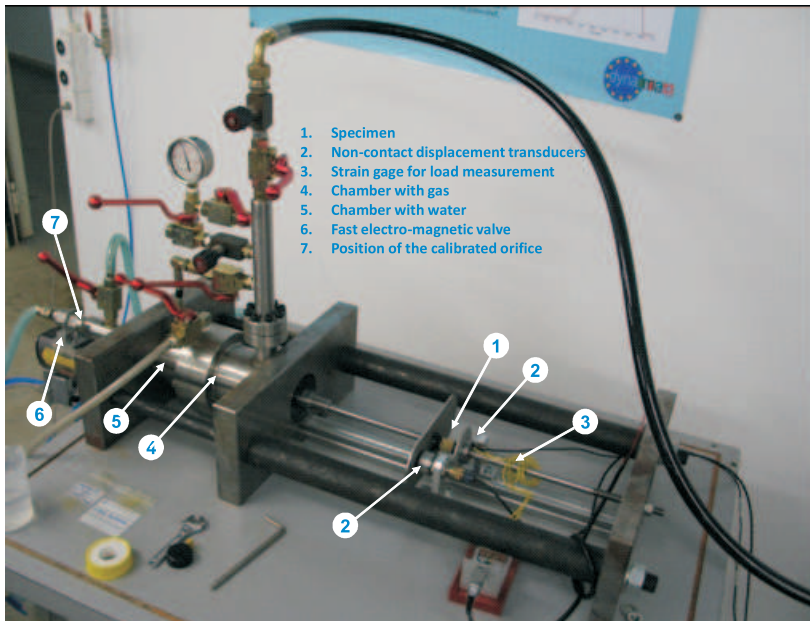


FIG. 4. Hydro-pneumatic machine used for medium strain-rate.

the water and gas chambers, so that forces acting on the two piston faces are in equilibrium. The test starts when the second chamber discharges the water through a calibrated orifice (7), activated by a fast electro-valve (6). Then, the piston starts moving expelling out the gas through a sealed opening; the end of the piston shaft is connected to the rock specimen (1); the specimen is linked to the piston shaft and to one end of an elastic bar (3), whose other end is rigidly fixed to a supporting structure. When the piston shaft moves, the specimen is pulled at a fixed strain-rate level, depending on the velocity of the gas expelling from the chamber. The elastic bar is instrumented with a strain-gauge (3) that provides, through the elastic properties of the bar, the force acting on the specimen during the test. Two targets are attached on both ends of the specimen and their movements are measured by two contact-less displacement transducers (2).

The constant speed movement of the piston guarantees the constancy of the strain-rate during the test; this depends mainly on the constancy of the force exerted by the gas pressure on the piston face. A good result in this sense was obtained with small change of gas volume during the test in order to have small gas pressure decrease and consequently small piston force decrease. Furthermore, the load  $P$  resisted by the specimen is measured by the dynamometric elastic bar, whereas the specimen elongation  $\Delta L$  is measured by the displacement transducers, sensing the displacement of the plates target fixed to both specimen ends. Such acquisitions allow to obtain the stress vs. strain relationship at the strain-rate level, achieved during the test.

#### 4. RESULTS AND DISCUSSION

The strain rate behaviour of the orthogneiss rock (for  $\theta = 0^\circ$ ,  $45^\circ$  and  $90^\circ$ ) and two marbles are here described with the results obtained by the two dynamic testing set-ups and the quasi-static results.

##### 4.1. High strain rate results

All results of the tests at high strain rate carried out by the JRC-SHTB are summarized in Table 2. All the tests have been performed keeping the preload constant (18 kN); in this way, the rocks were tested under the same loading condition. The strain rate behaviour of the orthogneiss has been analysed in three  $\theta$  orientations:  $\theta = 0^\circ$ ,  $\theta = 45^\circ$  and  $\theta = 90^\circ$ . The measurements of the strain histories of the input and output bars were used for determination of the stress versus strain curves by the Eqs. (3.1) and (3.2). In Fig. 5 are shown the stress versus strain curves of the orthogneiss (a) for  $\theta = 0^\circ$ ,  $\theta = 45^\circ$  and  $\theta = 90^\circ$  and the two Carrara and Peccia marbles (b). These diagrams con-

**Table 2. High strain rate results.**

Rock material	Dynamic Tensile Strength $f_{t,d}$ [MPa]	Average value $f_{t,d,ave}$ [MPa]	Fracture Energy $G_{f,d}$ [J/m <sup>2</sup> ]	Average value $G_{f,d,ave}$ [J/m <sup>2</sup> ]	Stress rate [GPa/s]
Orthogneiss $\theta = 0^\circ$ _N1	25.71		1260		1161
Orthogneiss $\theta = 0^\circ$ _N2	24.96	25.45±0.4	1146	1304±183	1151
Orthogneiss $\theta = 0^\circ$ _N6	25.70		1505		870
Orthogneiss $\theta = 45^\circ$ _N3	8.07		414		405
Orthogneiss $\theta = 45^\circ$ _N4	16.86	13.52±4.7	1154	868±397	788
Orthogneiss $\theta = 45^\circ$ _N7	15.65		1036		737
Orthogneiss $\theta = 90^\circ$ _N1	6.50		691		257
Orthogneiss $\theta = 90^\circ$ _N4	9.56	8.67±1.9	801	712±81	545
Orthogneiss $\theta = 90^\circ$ _N6	9.96		643		534
Peccia_Marble_N1	11.50		302		719
Peccia_Marble_N3	12.47	12.04±0.5	378	355±46	676
Peccia_Marble_N4	12.30		384		658
Carrara_Marble_N1	6.49		368		223
Carrara_Marble_N2	8.74	7.08±1.4	441	380±56	390
Carrara_Marble_N3	6.02		330		187

firm that the JRC-SHTB is able to measure both the ascending and descending branch of the curve and permits to measure the fracture energy (computed as the subtended area in a stress-displacement curve). For the orthogneiss analysed, the fracture energy changes with the orientation of schistosity at high strain rates. Higher values are observed for the  $\theta = 0^\circ$ , while lower values are for  $\theta = 90^\circ$ , then fracture energy reveals an increasing trend with the orientation. This increase in fracture energy shows that at  $\theta = 0^\circ$  this orthogneiss is more ductile [9]. In order to understand better the ductility and/or brittleness of this material, the characteristic length should be considered. As a unique material property, the characteristic length  $l_{ch} = G_F \cdot E / f_t^2$  expresses fracture of concrete-like materials, which is inversely proportional to the square of the tensile strength. This means that brittleness decreases with high fracture energy and increases with an increase of strength of the material. The values at  $\theta = 0^\circ$ ,  $\theta = 45^\circ$  and  $\theta = 90^\circ$  are respectively 79 mm, 192 mm and 413 mm [9]. The lower value is for  $\theta = 0^\circ$  revealing less brittle behaviour with respect to the other two ( $\theta = 90^\circ$  and  $\theta = 45^\circ$ ). The brittleness increases also with the strain rate [8].

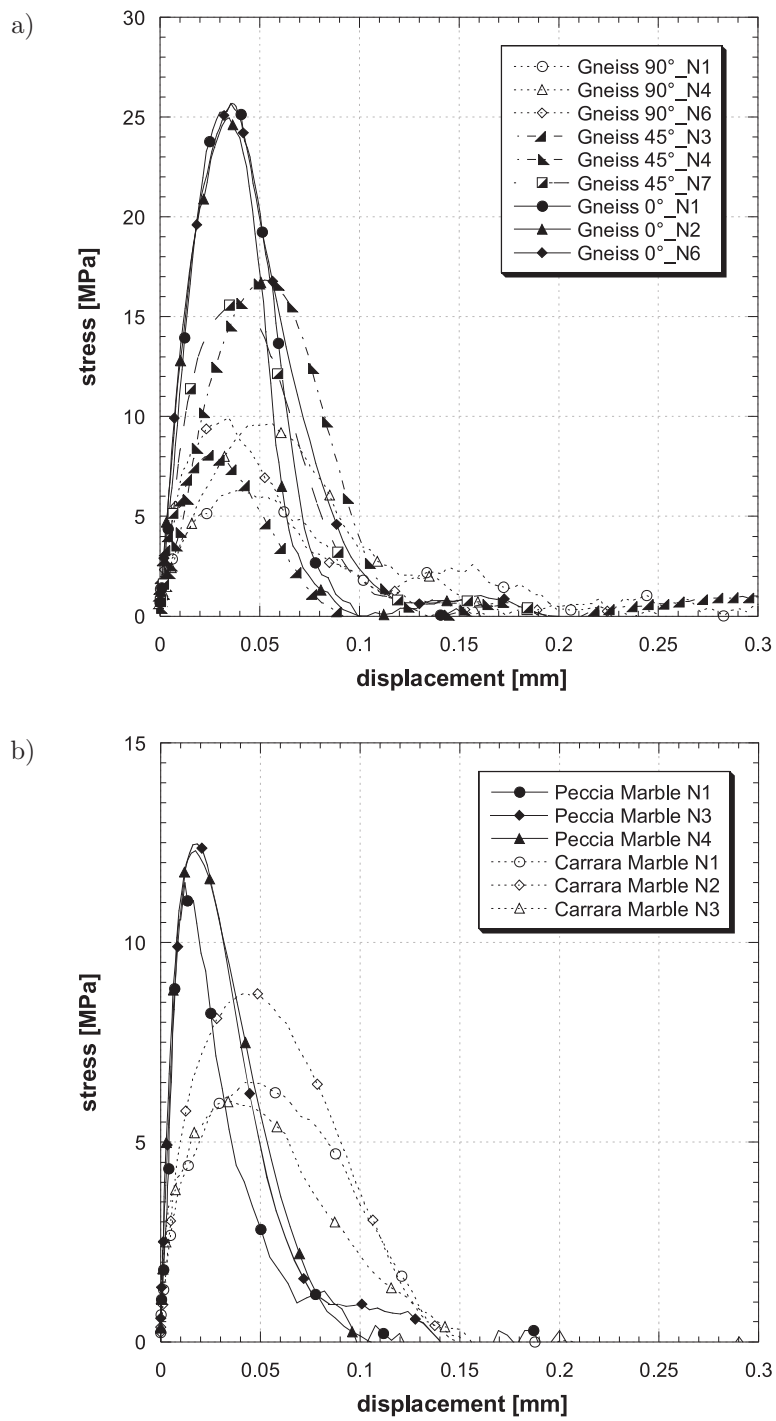


FIG. 5. Stress versus displacement curves of: a) orthogneiss, b) marbles.

In Fig. 6 are shown the photos of the Onsernone orthogneiss (a) and the Carrara marble (b) after the dynamic test with the JRC-SHTB.

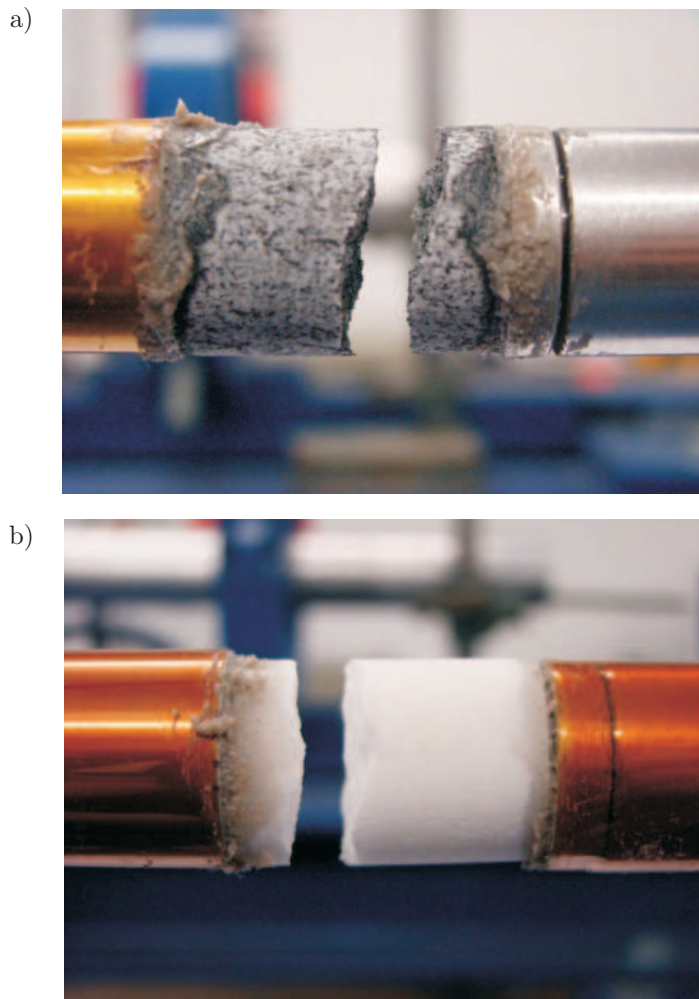


FIG. 6. Specimen after dynamic test: a) Orthogneiss, b) Carrara marble.

#### *4.2. Medium strain rate results*

The medium strain rate has been studied using a HPM with different calibrated orifices, having diameters from 1 mm to 3 mm. With the smaller diameter has been obtained lower intermediate velocity (about 200 MPa/s), while with the larger diameter has been obtained higher intermediate velocity (about 1500 MPa/s). The results are collected in Table 3. The tests have been carried out in tension for the same three  $\theta$  orientations  $0^\circ$ ,  $45^\circ$  and  $90^\circ$  of the orthogneiss.

**Table 3. Medium strain rate results.**

ID	Orifice diameter [mm]	Dynamic Tensile Strength $f_{t,d}$ [MPa]	Average $f_{t,d,ave}$ [MPa]	Stress rate obtained [GPa/s]
Orthogneiss $\theta = 0^\circ$ _N3	3	19.78		1.752
Orthogneiss $\theta = 0^\circ$ _N4	3	17.56	17.39±2.4	1.370
Orthogneiss $\theta = 0^\circ$ _N7	3	14.82		1.439
Orthogneiss $\theta = 0^\circ$ _N8	1	16.88		0.185
Orthogneiss $\theta = 0^\circ$ _N9	1	15.19	15.77±0.9	0.207
Orthogneiss $\theta = 0^\circ$ _N13	1	16.38		0.191
Orthogneiss $\theta = 45^\circ$ _N1	3	8.66		1.401
Orthogneiss $\theta = 45^\circ$ _N2	3	10.72	8.92±1.2	1.457
Orthogneiss $\theta = 45^\circ$ _N8	3	8.20		1.514
Orthogneiss $\theta = 90^\circ$ _N2	3	2.26		1.665
Orthogneiss $\theta = 90^\circ$ _N3	3	4.42	4.21±1.8	1.354
Orthogneiss $\theta = 90^\circ$ _N7	3	5.96		1.525
Orthogneiss $\theta = 90^\circ$ _N8	1	4.56		0.201
Orthogneiss $\theta = 90^\circ$ _N9	1	1.91	3.73±1.6	0.116
Orthogneiss $\theta = 90^\circ$ _N11	1	4.95		0.193
Carrara_Marble_N7	2	4.15		0.998
Carrara_Marble_N8	2	3.92		1.035
Carrara_Marble_N9	2	3.72		0.734
Carrara_Marble_N10	2	4.66	4.42±0.8	0.918
Carrara_Marble_N11	2	4.12		0.980
Carrara_Marble_N12	2	5.96		1.013
Peccia_Marble_N11	2	4.43		0.784
Peccia_Marble_N12	2	5.91	5.80±1.3	0.979
Peccia_Marble_N13	2	7.07		0.939

#### 4.3. Strain rate effect

Analysing the results at different strain rates it can be immediately observed that there is a dramatic difference in the strengths between the quasi-static and dynamic loading.

In Fig. 7 is shown the comparison between the static and dynamic stress versus displacement curves of Carrara Marble. For the rocks analysed, the dynamic strength at high strain rate is at least twice that of the static strength, indicating that rock reacts quite differently to dynamic loading than to static

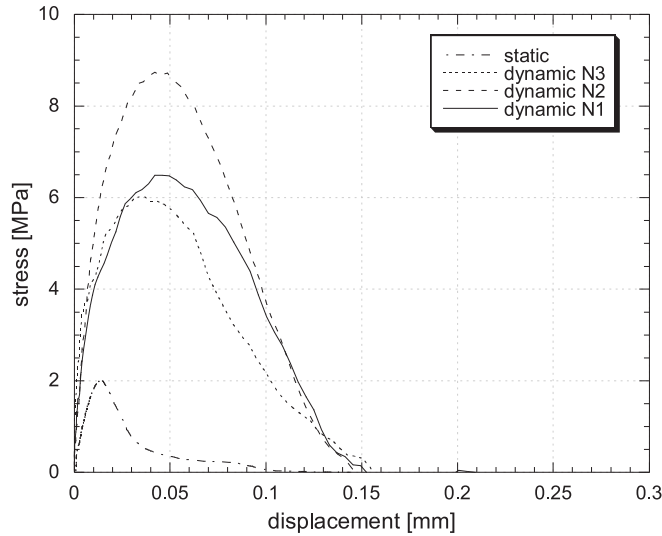


FIG. 7. Quasi-static and dynamic stress vs. displacement curves of Carrara Marble.

loading. The Carrara marble respond to the high loading rate with an increment of absorbed energy and larger deformation; all these effects can be attributed to the dynamic failure process.

The fracture processes of rocks are not the same under the static and dynamic types of loading as for concrete [5–7]. The rapid increase in terms of strength with increase in rate of loading has been explained through the impossibility for the weakest links in the rock to participate in the fracturing process. In fact, they may not necessarily have the time to propagate following the minimum energy path due to the nature of the dynamic fracturing process, that involves a complex interaction of multiple crack growth [6]. The test results show how the loading rate effect is governed by the wave propagation in the material in dynamic case (high strain rate), while in the quasi-static case the cracking process is governed by the defect and preferential plane of fracture eventually present in the rocks.

The strain-rate behaviour on the tensile strength can be represented through the ratio between the dynamic and static strength, well-known as Dynamic Increase Factor (DIF). It has been found that DIF of strength increase with strain rate. This ratio is usually higher for low strength rocks, and lower for high strength rocks.

DIF has been extensively used in order to quantify strain-rate effects for concrete-like materials in a large number of experimental researches. From these results some expressions of the DIF of the tensile strength have been developed but unfortunately, these do not consider any corrections taking into considera-

tion the type of materials (grain size, specimen size, etc.), neither the type of experimental set-up used to determine the dynamic tensile strength. In the case of compression [11] it is known that the dynamic strength of rocks at strain rates higher than  $10^2 \text{ s}^{-1}$  can be expressed as  $\sigma_d = K(d\varepsilon/dt)^{1/3}$ . In the case of tension, this assumption cannot be accepted because of fracture behaviour that strictly depends to the nature of the rocks.

Figure 8 illustrates the increase of the DIF versus strain rate, obtained by other researchers [9] and of the rocks here considered. It is shown that at lower strain rates, the strength increase is gradual above a certain strain rate, whilst this increase is drastic for higher strain rates. This transition seems to be present in the lower strength rocks and might be less marked for the higher strength rocks. This transition may be dependent on rock type and loading.

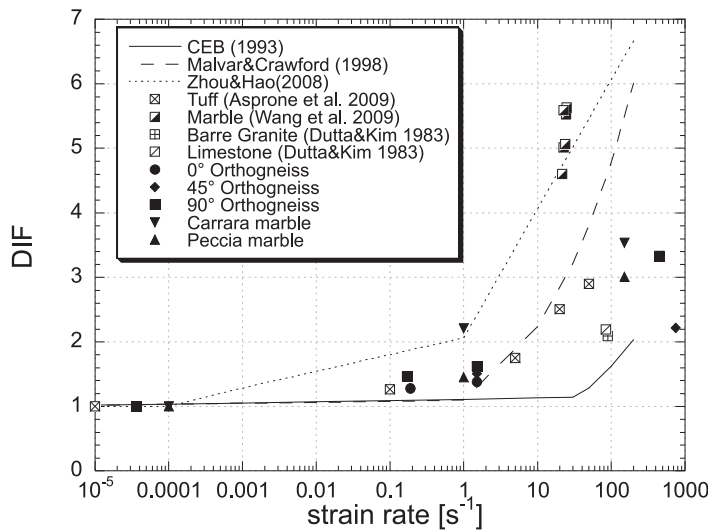


FIG. 8. DIF vs. strain rate.

In Fig. 8 are shown some formulations proposed for rocks and concrete [12], but it confirms that a more suitable formulation is necessary for rocks and that a wide experimental campaign on different families of rocks is needed.

## 5. CONCLUDING REMARKS

Dynamic direct tensile tests of an orthogneiss and two marbles were conducted using the JRC-Split Hopkinson Tensile Bar, and Hydro Pneumatic Machine for dynamic testing and an electro-mechanic machine for quasi-static tests. Results show that rock tensile strength is strain-rate dependent.

The mechanism of failure under dynamic loading by stress wave is significantly different from the quasi-static loading. Dynamic loading produces multiple fractures and this brings the material to absorb more energy, because higher loads are required to complete failure.

It has been verified that for the orthogneiss the tensile strength increases with the strain rate increasing within the wide strain rate range. The results show a non-linear relationships between strength and strain rates and the influence of the loading direction with respect to the schistosity of the orthogneiss examined. No influence were observed for the marbles.

Finally, the results confirm that a more appropriate formulation is necessary to describe the dynamic tensile strength evolution in function of the strain rate for rocks. Future research will be addressed to increase the knowledge on the dynamic behaviour of other rock types and in a wide range of strain rates using the experimental techniques presented here.

#### REFERENCES

1. A. J. ZIELINSKI, *Fracture of concrete and mortar under uniaxial impact tensile loading*, D.Sc. Thesis, Delft Univ., 1982.
2. H. W. REINHARDT, H. A. KÖRMELING, A. J. ZIELINSKI, *The split Hopkinson bar, a versatile tool for the impact testing of concrete*, *Materiaux et Constructions*, **19**, 1, 55–63, 1986.
3. J. R. KLEPACZKO, A. BRARA, *Experimental method for dynamic tensile testing of concrete by spalling*, *International Journal of Impact Engineering*, **25**, 387–409, 2001.
4. H. SCHULER, C. MAYRHOFER, K. THOMA, *Spall experiments for the measurement of the tensile strength and fracture energy of concrete at high strain rates*, *International Journal of Impact Engineering*, **32**, 1635–1650, 2006.
5. C. ALBERTINI, E. CADONI, K. LABIBES, *Dynamic mechanical behaviour of large concrete specimen by means of a bundle Hopkinson bars*, *Proc. 2nd Int. Sym. on Impact Engineering*, *Chinese Mechanics Journal*, Beijing, pp. 214–219, 1996.
6. C. ALBERTINI, E. CADONI, K. LABIBES, *Impact fracture process and mechanical properties of plain concrete by means of an Hopkinson bar bundle*, *Journal de Physique*, **7**, C3, 915–920, 1997.
7. E. CADONI, G. SOLOMOS, A. ALBERTINI, *Mechanical characterization of concrete in tension and compression at high strain-rate using a modified Hopkinson bar*, *Magazine of Concrete Research*, **61**, 3, 221–230, 2009.
8. D. ASPRONE, E. CADONI, A. PROTA, G. MANFREDI, *Dynamic behavior of a Mediterranean natural stone under tensile loading*, *International Journal of Rock Mechanics and Mining Sciences*, **46**, 514–520, 2009.
9. E. CADONI, *Dynamic Characterization of an Orthogneiss Rock Subjected to Intermediate and High Strain Rate in Tension*, *accepted for publication*, *Rock Mechanics and Rock Engineering*, 2010.

10. E. CADONI, M. DOTTA, D. FORNI, P. GIORGETTI, G. RIGANTI, C. ALBERTINI, *Mechanical characterization of rocks at high strain rate by the JRC modified Hopkinson bar: A tool in blast and impact assessment*, Rock Fragmentation by Blasting – Sanchidrián [Ed.], 2009, Taylor & Francis Group, London, ISBN 978-0-415-48296-7, pp. 35–41.
11. S. KUBOTA, Y. OGATA, Y. WADA, G. SIMANGUNSONG, H. SHIMADA, K. MATSUI, *Estimation of dynamic tensile strength of sandstone*, International Journal of Rock Mechanics and Mining Sciences, **45**, 397–406, 2008.
12. Comité Euro-International du Béton (1993), CEB-FIP Model Code 1990, Redwood Books, Trowbridge, Wiltshire, UK.

*Received January 20, 2011; revised version June 4, 2011.*

---